Volume 8
Number 46
14 December 2020
Pages 24217–24814

Journal of Materials Chemistry A

Materials for energy and sustainability

rsc.li/materials-a

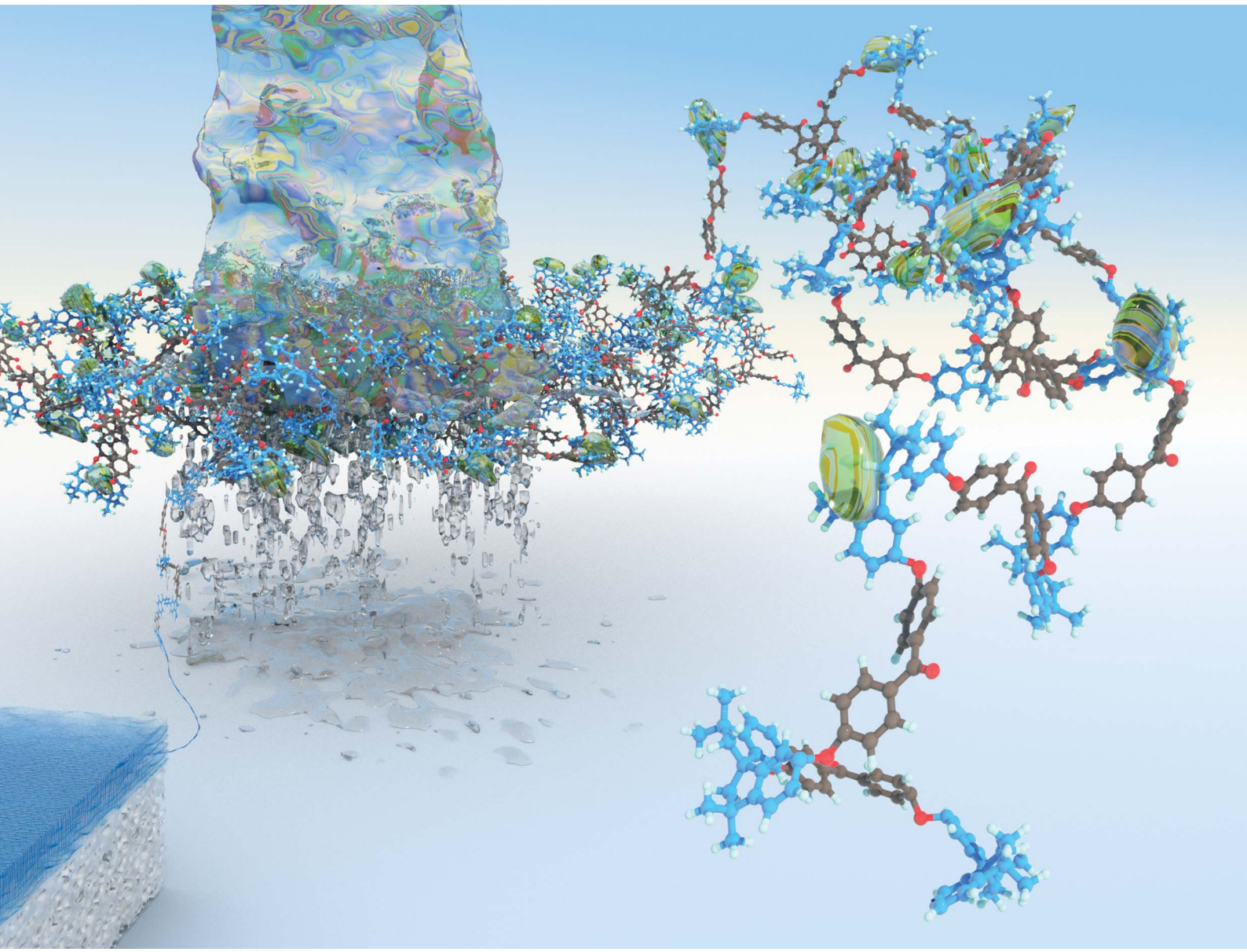

ISSN 2050-7488

ROYAL SOCIETY OF CHEMISTRY

PAPER

Gyorgy Szekely *et al.*
Molecular engineering of high-performance nanofiltration membranes from intrinsically microporous poly(ether-ether-ketone)

Journal of Materials Chemistry A

ROYAL SOCIETY OF CHEMISTRY

PAPER

View Article Online
View Journal | View Issue

Cite this: J. Mater. Chem. A, 2020, 8, 24445

Molecular engineering of high-performance nanofiltration membranes from intrinsically microporous poly(ether-ether-ketone)†

Mahmoud A. Abdulhamid, [a] Sang-Hee Park, [a] Hakkim Vovusha, [b] Faheem Hassan Akhtar, [c] Kim Choon Ng, [c] Udo Schwingenschlögl [b] and Gyorgy Szekely *[a]

Poly(ether-ether-ketone) has received increased attention due to its high thermal and chemical stability, and high performance in various applications. However, it suffers from a semi-crystalline morphology, low fractional free volume, and poor processability, requiring the use of harsh acidic solvents, which leads to undesired sulfonation. In this work, three intrinsically microporous poly(ether-ether-ketones) (iPEEKs), incorporating spirobisindane, Tröger's base, and triptycene contorted structures, were developed for organic solvent nanofiltration. Molecular dynamics simulations have assisted the molecular engineering of the polymers and the understanding of the improved membrane performance through the binding energies between solvents and polymers. Application of the design principles of polymers of intrinsic microporosity has led to a paradigm shift with a notable enhancement in both the polymer properties and the subsequently fabricated nanofiltration membranes' performance. The iPEEKs showed excellent solution processability, a high surface area of 205–250 $m^2\ g^{-1}$, and excellent thermal stability. Mechanically flexible nanofiltration membranes were prepared from *N*-methyl-2-pyrrolidone dope solution at iPEEK concentrations of 19–35 wt%. The molecular weight cutoff of the membranes was fine-tuned in the range of 450–845 g mol^{-1} displaying 2–6 fold higher permeance (3.57–11.09 L $m^{-2}\ h^{-1}\ bar^{-1}$) than previous reports. The long-term stabilities were demonstrated by a 7 day continuous cross-flow filtration.

Received 20th August 2020
Accepted 6th October 2020

DOI: 10.1039/d0ta08194a

rsc.li/materials-a

Introduction

Organic solvent nanofiltration (OSN) is an energy-efficient separation technology that can distinguish solute concentrations in the range of 100–2000 g mol^{-1} using solvent-resistant membranes in organic media.[1,2] OSN has found numerous applications in the petrochemical and fine chemical industries, such as product or catalyst purification and recovery, and solvent recycling or exchange. One of the key challenges in OSN is to develop new membrane materials with improved performance, manifested in higher permeance, better selectivity, and better chemical and thermal stability.

Poly(ether-ether-ketone) (PEEK) has attracted the attention of membrane scientists in recent years due to its excellent solvent resistance and thermal stability.[3–8] PEEK is a semi-crystalline polymer with very low fractional free volume (FFV). PEEK is insoluble in organic solvents and can only be dissolved in methanesulfonic acid (MSA) and sulfuric acid (SA).[6] However, this advantage of OSN applicability results in poor processability. The harsh acidic conditions required for making PEEK membranes are undesirable, and also lead to the unavoidable sulfonation of the polymer. The degree of sulfonation can be minimized to less than 7% by using a solvent mixture of MSA and SA (3 : 1) at 20 °C.[5] Nonetheless, the presence of $-SO_3H$ groups adversely affects the properties of the membrane materials by decreasing the chemical and thermal stability, the adsorption of solutes, and even the potential to transform fine chemicals.[9,10]

A previously proposed solution includes converting the carbonyl group of the PEEK to a ketal in a two-step synthesis and fabricating a membrane from the resulting soluble precursor, followed by an acid treatment, thus allowing the retention of the original PEEK structure.[8] In another approach,

[a]Advanced Membranes and Porous Materials Center, Physical Science and Engineering Division (PSE), King Abdullah University of Science and Technology (KAUST), Thuwal, 23955-6900, Saudi Arabia. E-mail: gyorgy.szekely@kaust.edu.sa; Web: www.szekelygroup.com

[b]Physical Science and Engineering Division (PSE), King Abdullah University of Science and Technology (KAUST), Thuwal, 23955-6900, Saudi Arabia

[c]Water Desalination and Reuse Center, King Abdullah University of Science and Technology, Thuwal 23955-6900, Saudi Arabia

† Electronic supplementary information (ESI) available: Materials and methods; instrumental procedures; NMR, FTIR spectra; DSC, BET, nanoindentation graphs; SEM, AFM images; filtration tests, swelling experiments and MD simulation. See DOI: 10.1039/d0ta08194a

carboxylic acid moieties were introduced into the PEEK framework, which improved its solubility and allowed crosslinking of the resulting membrane.[11] The negligible aging of PEEK in organic solvents was also recently demonstrated, which triggered further interest in this class of polymers for OSN applications.[7]

Polymers of intrinsic microporosity (PIMs) have emerged as high surface area, thermally stable, solution-processable polymers.[12] The design concept of these materials is based on the insertion of non-planar, contorted structures into a polymer backbone that can inhibit polymer chain packing, and therefore increase the FFV of the material.[13–15] A plethora of applications have successfully exploited PIMs, including gas separation,[16] hydrogen storage,[17] sensors,[18] electrochemistry,[19] catalysis,[20] and printed electronics.[21] PIM-1 is the first choice for the preparation of OSN membranes, either unmodified,[22–24] modified,[25] or as a polymer blend.[26] Subsequent studies have also explored PIM-7 and PIM-8.[27] In general, these membranes demonstrate (i) high permeance compared to non-intrinsically porous polymer membranes, and (ii) a wide range of molecular weight cut-off (MWCO) values between 190 and 650 g mol^{-1}.[26,28–30] Consequently, both PIM and PEEK have great potential as engineering membrane materials, and herein their molecular fusion into intrinsically microporous poly(ether-ether-ketone) (iPEEK) is explored. Three solution-processable iPEEKs were prepared by the nucleophilic aromatic substitution reaction using three different contorted monomers and 4,4′-difluorobenzophenone (Scheme 1). The phenyl ring in the commercial PEEK was substituted by three different kinked structures, namely spirobisindane (SBI), Tröger's base (TB), and triptycene (Trip), resulting in iPEEK-SBI, iPEEK-TB, and iPEEK-Trip, respectively.

Experimental

Monomer synthesis

Synthesis of 3,3,3′,3′-tetramethyl-2,2′,3,3′-tetrahydro-1,1′-spirobi[indene]-6,6′-diol (SBI) (2). 4,4′-Isopropylidenediphenol (Bisphenol A) (20 g, 88 mmol) and methanesulfonic acid (3 ml) were mixed and heated at 135 °C for 2.5 h. The obtained brown sticky oil was poured onto iced water and left to stir for an hour before filtering the fine brown powder. White powder (6.3 g, 70% yield) was obtained after recrystallizing the crude product by water/methanol (60/40, wt/wt). Further purification was done to obtain a high purity product for the polymerization reaction. ^{1}H NMR (400 MHz, DMSO-d_6, δ): 1.25 (s, 6H), 1.32 (s, 6H), 2.09–2.12 (d, 2H, J = 12.92 Hz), 2.24–2.28 (d, 2H, J = 12.96 Hz), 6.11 (d, 2H, J = 2.24 Hz), 6.6 (dd, 2H, J = 8.16 Hz), 7.0 (d, 2H, J = 8.16 Hz), 9.01 (s, 2H). ^{13}C NMR (100 MHz, DMSO-d_6, δ): 31, 32.1, 42.8, 57.4, 59.8, 110.4, 114.8, 122.8, 142.6, 151.9, 157.2; MS-HESI

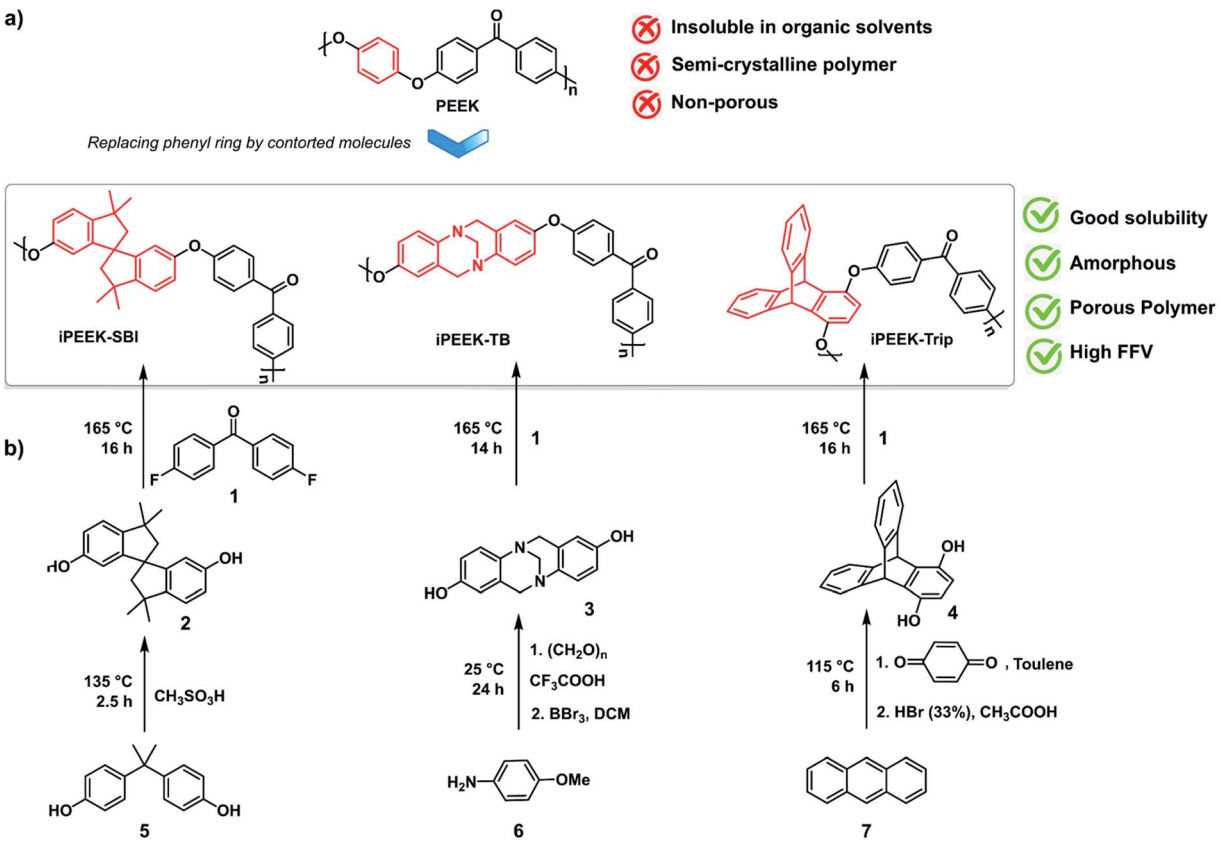

Scheme 1 (a) The concept of molecular fusion of PEEK and PIM into intrinsically microporous poly(ether-ether-ketone) (iPEEK) by the substitution of the phenyl ring in PEEK by contorted structures to enhance the fractional free volume (FFV), porosity and the solution-processability. (b) Synthetic route for the contorted, diol monomers and their corresponding polymers.

(m/z): [M + CH_3COO^-] calcd for [$C_{21}H_{24}O_2$ + CH_3COO^-]: 367.19; found: 367.00.

Synthesis of 6*H*,12*H*-5,11-methanodibenzo[*b*,*f*][1,5]diazocine-2,8-diol (TB) (3). *p*-Anisidine (10 g, 82.5 mmol) was added to a 500 ml dry round bottom flask, followed by the addition of 80 ml CF_3COOH and paraformaldehyde at room temperature. The reaction was left to stir for 24 h before pouring it onto iced water and ammonium hydroxide solution. The pH of the medium was adjusted to 6, and the obtained precipitates were collected by filtration. A silica gel column was used to further purify this intermediate using hexane/ethyl acetate: 1/2 as the eluent to obtain dimethoxy Tröger's base as light yellow crystals (8 g, 70% yield).

The dry dimethoxy Tröger's base (7 g, 24.8 mmol) was dissolved in anhydrous dichloromethane and cooled down to 0 °C. BBr_3 was added dropwise and then the reaction was left to stir overnight at room temperature. The reaction mixture was poured onto water and stirred for 6 hours under nitrogen flushing, before adjusting the pH of the medium between 5 and 6 using 10% of Na_2CO_3. The obtained precipitates were collected and dried in the oven at 110 °C for 24 hours to afford a white solid (5.5 g, 90%). ^{1}H NMR (400 MHz, DMSO-d_6, δ): 3.88 (d, 2H, J = 16.72 Hz), 4.1 (s, 2H), 4.45 (d, 2H, J = 16.68 Hz), 6.30 (d, 2H, J = 2.52 Hz), 6.54 (dd, 2H, J = 8.6 Hz), 6.88 (d, 2H, J = 8.6 Hz). ^{13}C NMR (100 MHz, DMSO-d_6, δ): 58.7, 67.2, 112.6, 114.8, 126, 129.2, 140, 153.7. MS-HESI (m/z): [M + H]$^+$ calcd for [$C_{15}H_{15}N_2O_2$]$^+$: 255.11; found 255.00.

Synthesis of (9*s*,10*s*)-9,10-dihydro-9,10-[1,2]benzenoanthracene-1,4-diol (Trip) (4). Antharacene (35.65 g, 200 mmol) and benzoquinone (21.63 g, 200 mmol) were refluxed in toluene at 115 °C for 6 hours and then cooled down to RT. Triptycenequinone was precipitated as a greenish-yellow precipitate which was collected by filtration and washed a few times by toluene. The obtained crude product was placed in the vacuum oven at 75 °C for 6 hours. 45 grams (79% yield) of the triptycenequinone was obtained and used without any further purification for the second step, in which 45 grams was suspended in 300 ml glacial acetic acid and heated it to reflux 118 °C. Then 1.4 ml (33% HBr) was added drop wise to the solution and then left to stir for 3 minutes at reflux. The system was cooled down and filtered then washed with toluene and placed in the oven at 100 °C for 18 hours. 80% yield was obtained. Further purification was done to afford white crystals with high purity for the polymerization reaction. ^{1}H NMR (400 MHz, DMSO-d_6, δ): 5.81 (s, 2H), 6.32 (s, 2H), 6.98 (m, 4H), 7.40 (m, 4H), 8.83 (s, 2H). ^{13}C NMR (100 MHz, DMSO-d_6, δ): 47.1, 113.4, 124, 125.1, 132.4, 145.3, 146.3. MS-HESI (m/z): [2M − H$^+$] calcd for [$2C_{20}H_{14}O_2$ − H$^+$]: 571.20; found: 571.00.

Polymer synthesis

As shown in Scheme 1, iPEEK-SBI, iPEEK-TB and iPEEK-Trip were prepared by a one-step high-temperature aromatic nucleophilic substitution reaction (S_NAr) using an equimolar amount of the commercially available 4,4′-difluorobenzophenone and the corresponding diol compounds (*i.e.* SBI, TB, and Trip) in DMAc and in the presence of K_2CO_3. The general procedure of this polymerization reaction is as follows: 4,4′-difluorobenzophenone and the diol compounds were added to a two-necked 200 ml round bottom flask equipped with a Dean–Stark apparatus under a nitrogen atmosphere. The reagents were dissolved in anhydrous DMAc and anhydrous toluene (4/1: DMAc/toluene). 1.2 equivalent of K_2CO_3 was added and the reaction was heated to 140 °C and kept for a few hours for azeotropic distillation to completely remove water that was produced during the reaction. After total collection of toluene, the reaction was then heated to 165 °C and left for about 14–16 hours. Then the reaction mixture was then poured into distilled water and stirred for 6 hours, filtered and then refluxed for 24 hours with water, and 24 hours with methanol before drying in a vacuum oven at 180 °C for 24 hours. The polymers were fully characterized by ^{1}H NMR, FT-IR, GPC, and Brunauer–Emmett–Teller (BET) surface area analysis and demonstrated good solution processability, which allowed the fabrication of robust membranes using the phase inversion method.

iPEEK-SBI. Yield: 94%. ^{1}H NMR (500 MHz, $CDCl_3$, δ): 1.37 (s, 6H), 1.38 (s, 6H), 2.26–2.29 (d, 2H, J = 15 Hz), 2.40–2.43 (d, 2H, J = 15 Hz), 6.56 (d, 2H, J = 2.1 Hz), 6.89 (dd, 2H, J = 6.9 Hz), 6.94 (d, 4H, J = 8.55 Hz), 7.14 (d, 2H, J = 8.2 Hz), 7.71 (d, 4H, J = 8.65 Hz). ^{13}C NMR (125 MHz, $CDCl_3$, δ): 30.3, 31.8, 43.2, 57.6, 59.6, 115.9, 116.6, 119.2, 123.2, 131.9, 132.2, 148.5, 152.3, 154.8, 161.7, 194.1; FT-IR (ν, cm^{-1}): 2950–3000 (C–H, str), 1655 (C═O *asym*, str), 1596 (C═O *sym*, str), 1229 (C–O, str); M_n = 40 000 g mol^{-1}; PDI = 2.60; ρ = 1.161 g ml^{-1}; S_{BET} = 205 m^2 g^{-1}; TGA analysis: $T_{d,5\%}$ = 495 °C.

iPEEK-TB. Yield: 90%. ^{1}H NMR (500 MHz, $CDCl_3$, δ): 4.15 (d, 2H, J = 15 Hz), 4.37 (s, 2H), 4.72 (d, 2H, J = 15 Hz), 6.68 (s, 2H), 6.92–6.98 (m, 6H), 7.2 (d, 2H, J = 7.65 Hz), 7.75 (d, 4H, J = 6.85 Hz). ^{13}C NMR (125 MHz, $CDCl_3$, δ): 58.4, 66.8, 117.2, 117.4, 118, 119.6, 126.6, 129, 132.2, 132.3, 143.4, 152.2, 161.3, 194.1; FT-IR (ν, cm^{-1}): 2846–2969 (C–H, str), 1652 (C═O *asym*, str), 1596 (C═O *sym*, str), 1235 (C–O, str); M_n = 49 600 g mol^{-1}; PDI = 1.92; ρ = 1.302 g ml^{-1}; S_{BET} = 220 m^2 g^{-1}; TGA analysis: $T_{d,5\%}$ = 405 °C.

iPEEK-Trip. Yield: 96%. ^{1}H NMR (500 MHz, $CDCl_3$, δ): 5.62 (s, 2H), 6.79 (s, 2H), 6.95 (d, 4H, J = 8.65 Hz), 6.99 (m, 4H), 7.24 (m, 4H), 7.85 (d, 4H, J = 8.6 Hz); ^{13}C NMR (125 MHz, $CDCl_3$, δ): 48.2, 116.2, 119.5, 124.1, 125.5, 132.1, 132.4, 146.5, 161.9, 194.1; FT-IR (ν, cm^{-1}): 1655 (C═O *asym*, str), 1596 (C═O *sym*, str), 1222 (C–O, str); M_n = 40 700 g mol^{-1}; PDI = 3.17; ρ = 1.261 g ml^{-1}; S_{BET} = 250 m^2 g^{-1}; TGA analysis: $T_{d,5\%}$ = 526 °C.

Membrane fabrication

The iPEEKs were dissolved at different concentrations (Table 2) in NMP by overhead mechanical stirring (IKA® RW 20 digital) at 22 °C (Fig. 1). The dope solutions were then placed in an IKA® KS 4000 incubator shaker for 24 h at 22 °C to degas the solution. The dope solution was poured onto a Novatex 2471 polypropylene non-woven support (Freudenberg Filtration Technologies, Germany). A bench top casting machine (Elcometer 4340 Automatic Film Applicator) was used to cast a film using a blade film applicator (Elcometer 3700) set at 250 μm thickness, with a transverse speed of 150 m h^{-1}. The temperature was 22 °C with a relative humidity of 56%. The membrane was

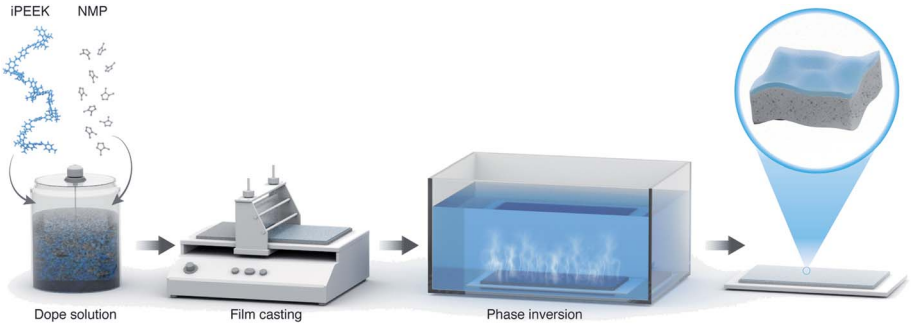

Fig. 1 Schematic overview of iPEEK membrane preparation through the phase inversion method.

phase inverted immediately by immersion in deionized Type II water with resistivity of 18.2 MΩ cm sourced from a Milli-Q Reference. The DI water in the bath was changed three times, finally the membranes were cut and saved in DI water with 1 vol% acetonitrile to prevent any bacterial growth. Refer to Section 1.2 of the ESI† for the membrane testing.

Polymer and membrane characterization

^{1}H and ^{13}C NMR spectra of the synthesized monomers and polymers were recorded with a Bruker AVANCE-III spectrometer at a frequency of 400 MHz in either deuterated chloroform ($CDCl_3$) or deuterated dimethylsulfoxide (DMSO-d_6) and recorded in ppm. Molecular weight and molecular weight distribution (PDI) of iPEEK-SBI, iPEEK-TB and iPEEK-Trip were obtained by high temperature (140 °C) gel permeation chromatography (GPC) (Agilent PL-GPC 220) using trichlorobenzene as a solvent and polystyrene as an external standard. FT-IR of the obtained membranes were acquired using a Varian 670-IR FT-IR spectrometer. Thermal gravimetric analysis (TGA) was carried out using a TGA Q5000 (TA Instruments); all analyses entailed a drying step at 100 °C for 30 min followed by a ramp of 5 °C min^{-1} to 800 °C. The glass transition temperature of all iPEEK polymers were obtained *via* differential scanning calorimetry (DSC) (TA Instruments, Model Q2000) with a ramp rate of 10 °C min^{-1} to 500 °C. The d-spacing between the polymer chains were measured by wide-angle X-ray scattering which is conducted on a Bruker D8 Advance diffractometer from 8 to 50° with a scanning rate of 0.5° min^{-1}. The surface and cross-sectional images of membranes were collected using scanning electron microscopy (SEM Merlin, ZEISS) which is operated at 5 kV with 5 mm of the working distance. The samples for the cross-sectional image were prepared by fracturing the frozen membranes in liquid nitrogen. All membranes were sputter-coated with 5 nm of iridium. The dried membranes were fixed on a slide glass using a both-side tape to obtain its flat surface. Surface roughness of the iPEEK membranes were obtained from an atomic force microscope (AFM, Agilent 5500) and calculated as an average of four times scanning, 5 × 5 μm images were taken and plotted in the ESI.† The swelling ratio (SR) was calculated from:

$$\mathrm{SR}\ (\%) = \frac{(L_{\mathrm{water}} - L_{\mathrm{solvent}})}{L_{\mathrm{water}}} \times 100 \qquad (1)$$

where L_{water} and L_{solvent} represent the thickness of the membrane soaked in water and selected solvents (24 h), respectively. Water contact angles of membranes were measured by the sessile drop method using a drop shape analyzer (Easy drop, KRUSS) equipped with a video camera. The average values were obtained from at least five measurements for each sample. The carbon dioxide adsorption isotherms of the powder samples of the three polymers were performed by using a surface area and porosimetry analyzer (Micrometrics ASAP 2050) at zero degrees up to 10 bar after degassing the samples at 180 °C for 12 h with pressure lower than 10 μmHg. The apparent BET surface area was calculated from CO_2 adsorption data by multi-point BET analysis.

A Mettler-Toledo balance equipped with a density measurement kit was used to determine the polymer density based on the buoyancy method using iso-octane as the reference liquid. Water vapor sorption was conducted as a function of relative humidity at 25 °C using a gravimetric sorption analyzer on Q5000-SA (TA Instruments, USA). The membrane samples were dried inside the sorption analyzer at 70 °C for 3 h to attain a constant weight prior to the sorption measurements. Sorption measurements were recorded at different relative humidity in the range from 0 to 95% relative humidity. Once the vapor uptake reached a certain humidity, it was equilibrated for at least 3 h to ensure steady state data. The mechanical properties were obtained using Nano Test Vantage instrument. The dried membranes were fixed on a silicon wafer surface and the test was done three times for each membrane to confirm the obtained results.

Results and discussion

Molecular design and synthesis

The iPEEKs were prepared by a one-step, high-temperature aromatic nucleophilic substitution reaction (S_NAr) between 4,4′-difluorobenzophenone (**1**) and three diol compounds (**2–4**) in the presence of anhydrous K_2CO_3 in anhydrous DMAc at 165 °C (Scheme 1). The chemical structures of the monomers and polymers were confirmed by ^{1}H and ^{13}C nuclear magnetic resonance (NMR) (Fig. S2–S13†) and mass spectroscopy (MS). Fourier transform infrared (FTIR) spectroscopy was used to detect the characteristic absorption bands for the iPEEKs (Fig. 2a). The ether linkage was obtained at 1229 cm^{-1} (C–O, str)

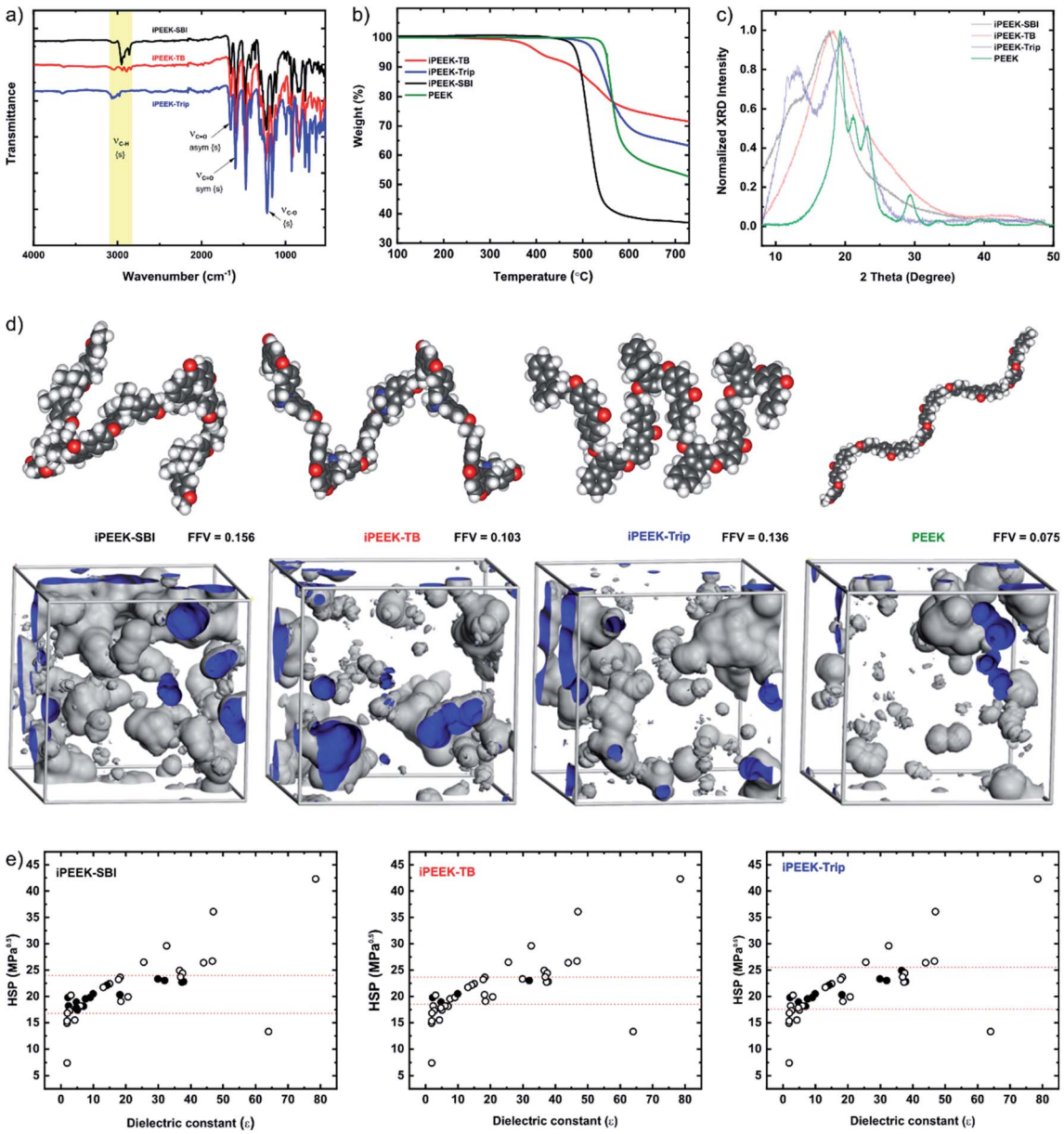

Fig. 2 Characterization of iPEEK-SBI, iPEEK-TB, and iPEEK-Trip: (a) Fourier transform infrared (FTIR) spectra. (b) Thermogravimetric analysis (TGA) under a N_2 atmosphere. (c) X-ray diffraction (XRD) spectra. (d) Calculated fractional free volumes (FFV) and geometry optimized 3D structures of the polymers obtained from Materials Studio software. (e) Polymer solubility as a function of the Hildebrand solubility parameter (HSP) *versus* the dielectric constant of organic solvents. The filled and empty circles refer to the polymers being soluble and insoluble in the given solvent, respectively (see also Tables S2–S9†).

and the keto group was obtained at 1655 cm^{-1} (C═O *asym*, str), and 1596 cm^{-1} (C═O *sym*, str). The thermogravimetric analysis (TGA) confirmed high thermal stability for all polymers (Fig. 2b, Table 1). In particular, the decomposition temperature values for iPEEK-SBI ($T_{d,5\%}$ = 495 °C) and iPEEK-Trip ($T_{d,5\%}$ = 526 °C) were comparable with the commercial PEEK ($T_{d,5\%}$ = 550 °C), while iPEEK-TB ($T_{d,5\%}$ = 405 °C) showed a moderate decrease due to the early decomposition of the Tröger's base bridge.[31] The glass transition temperatures (T_g) of the polymers, obtained by differential scanning calorimetry (DSC), were significantly higher than that of the conventional PEEK (T_g = 143 °C). For instance, iPEEK-Trip displayed the highest T_g of 256 °C, followed by iPEEK-SBI of 243 °C, and iPEEK-TB of 197 °C (Fig. S14–S16†). For the novel polymers, high-temperature gel permeation chromatography (GPC) was used to measure the number average molecular weight (M_n) and the polydispersity index (PDI). The three polymers revealed the high M_n value and moderate PDI. iPEEK-SBI, iPEEK-TB, and iPEEK-Trip showed M_n of 40 000 g mol^{-1}, 49 600 g mol^{-1}, and 40 700 g mol^{-1} with PDI values of 2.6, 1.98 and 3.17, respectively.

The solution processability of the polymers was improved by replacing the hydroquinone monomer (which is used for

Table 1 Physical properties of the iPEEKs and their comparison to those of the commercial PEEK

Polymer	M_w[a] (g mol^{-1})	M_n[a] (g mol^{-1})	PDI[a]	$T_{d,5\%}$[b] (°C)	T_g[c] (°C)	S_{BET} (m^2 g^{-1})	Density[d] (g cm^{-3})
iPEEK-SBI	104 600	40 000	2.60	495	243	205 ± 7	1.161 ± 0.004
iPEEK-TB	98 000	49 600	1.98	405	197	220 ± 10	1.302 ± 0.027
iPEEK-Trip	129 200	40 700	3.17	526	256	250 ± 6	1.261 ± 0.01
PEEK[5]	—	39 000	—	550	143	27 ± 5	1.3

[a] Measured by high temperature GPC with polystyrene as the calibration standard and trichlorobenzene as a solvent at 140 °C. [b] Measured by TGA with a ramp rate of 3 °C min^{-1} to 800 °C. [c] Measured by DSC with a ramp rate of 10 °C min^{-1}. [d] Measured using Archimedes principle and the Metler Toledo density kit in iso-octane solution.

commercial PEEK synthesis) with contorted structures (Fig. 2e, Tables S2–S9†). PEEK is insoluble in organic solvents and can only be dissolved in strong acids such as H_2SO_4, whereas iPEEKs are soluble in some organic solvents. Plotting the Hildebrand solubility parameters (HSPs) of the solvents as a function of their dielectric constant showed that iPEEKs are soluble in some solvents that have HSPs between 17 and 25 MPa$^{0.5}$ and dielectric constant between 0 and 40. In contrast, the polymers are insoluble in solvents that have HSPs lower than 17 and higher than 25 MPa$^{0.5}$ and dielectric constant above 40. Commercial PEEK demonstrates a semi-crystalline morphology, which governs the chain packing, leading to very low FFV (Fig. 2d) and thus very poor solubility. In this work, the semi-crystalline polymer was converted to an amorphous morphology and thus the solubility (Fig. 2e) and the FFV were enhanced by up to 104% (Fig. 2d) at the same time, by incorporating kinked structures that prevented the packing of polymer chains, thereby enhancing the porosity.

The wide-angle X-ray diffraction (WXRD) results demonstrated that incorporating SBI, TB, or Trip monomers led to an amorphous morphology and increased the d-spacing, confirmed by the peaks shifting toward lower 2 theta by 2 degrees (Fig. 2c and Table S10†). The obtained results were consistent with the BET surface area and the predicted FFV from MD simulations. The BET surface area of iPEEK was about 7–10 fold higher than that of PEEK at 27 m^2 g^{-1} (Fig. S17 and S18†). The FFV values of iPEEKs were found to be 0.103, 0.136, and 0.156 as a result of substituting the phenyl ring of PEEK (FFV = 0.075) by TB, Trip, and SBI, respectively. Dope solutions of the novel polymers, having different concentrations, were used to fabricate OSN membranes.

Membrane fabrication and characterization

Three series of nanofiltration membranes were prepared by phase inversion of the polymer dope solutions. The membranes are distinguished as: open (iPEEK-X^o), with the lowest polymer concentration and dope solution viscosity; ajar (iPEEK-X^a), with medium polymer concentration and dope solution viscosity; and tight (iPEEK-X^t), with the highest polymer concentration and dope solution viscosity (Table 2 and Fig. S19†). In the membrane designation, X refers to the polymer series, which are SBI, TB and Trip. The FTIR spectra of the nine membranes were identical to that of the polymer powders, as shown in Fig. S20,† proving that there were no changes in the molecular structure of the polymer after phase inversion. The iPEEK dope solutions were prepared in a way that the resulting viscosities fall within the same range for performance comparison purposes (Fig. S19†). The thickness of the polymer layer was obtained from the SEM cross-sectional images for the nine iPEEK membranes with increasing values from 67 to 151 μm as a function of increasing viscosity of the dope solutions.

Nanoindentation revealed that the membranes have good mechanical properties, flexibility, and a high reduced modulus, as shown in Table 2 and Fig. S21–S24.† For instance, taking the tightest membrane series as an example, iPEEK-Trip^t displayed

Table 2 Dope solution viscosity and concentration, membrane thickness and surface properties. There are membranes with 3 different polymer series: SBI, TB and Trip; and each polymer series can be broken down into 3 further series based on the tightness of the membranes: open (^{o}), ajar (^{a}) and tight (^{t}). The latter designation corresponds to the increase in the dope solution viscosity. See also ESI Fig. S19

				Surface properties			
Membrane	Viscosity (cP)	Concentration (wt%)	Thickness (μm)	Reduced modulus (GPa)	Hardness (GPa)	Contact angle (°)	Roughness, R_q (nm)
iPEEK-SBI^o	6737 ± 15	27	107 ± 4	0.513 ± 0.069	0.0053 ± 0.002	90 ± 2	8.97 ± 1.26
iPEEK-SBI^a	7704 ± 18	31	117 ± 6	0.953 ± 0.143	0.0455 ± 0.016	93 ± 1	5.82 ± 0.53
iPEEK-SBI^t	9927 ± 24	35	145 ± 3	0.892 ± 0.072	0.0175 ± 0.001	95 ± 1	4.40 ± 0.36
iPEEK-TB^o	6481 ± 17	19	133 ± 3	0.725 ± 0.034	0.0556 ± 0.009	83 ± 1	5.24 ± 0.35
iPEEK-TB^a	7454 ± 22	23	138 ± 1	0.762 ± 0.127	0.0176 ± 0.002	90 ± 2	4.21 ± 0.42
iPEEK-TB^t	9516 ± 23	27	151 ± 2	0.703 ± 0.024	0.0263 ± 0.002	95 ± 1	3.89 ± 0.61
iPEEK-Trip^o	6660 ± 19	26	67 ± 3	0.929 ± 0.127	0.0145 ± 0.001	71 ± 2	5.63 ± 0.71
iPEEK-Trip^a	7592 ± 21	30	100 ± 4	1.153 ± 0.029	0.0326 ± 0.002	75 ± 2	4.74 ± 0.51
iPEEK-Trip^t	9803 ± 26	34	112 ± 2	1.114 ± 0.04	0.0292 ± 0.001	78 ± 1	3.94 ± 0.50

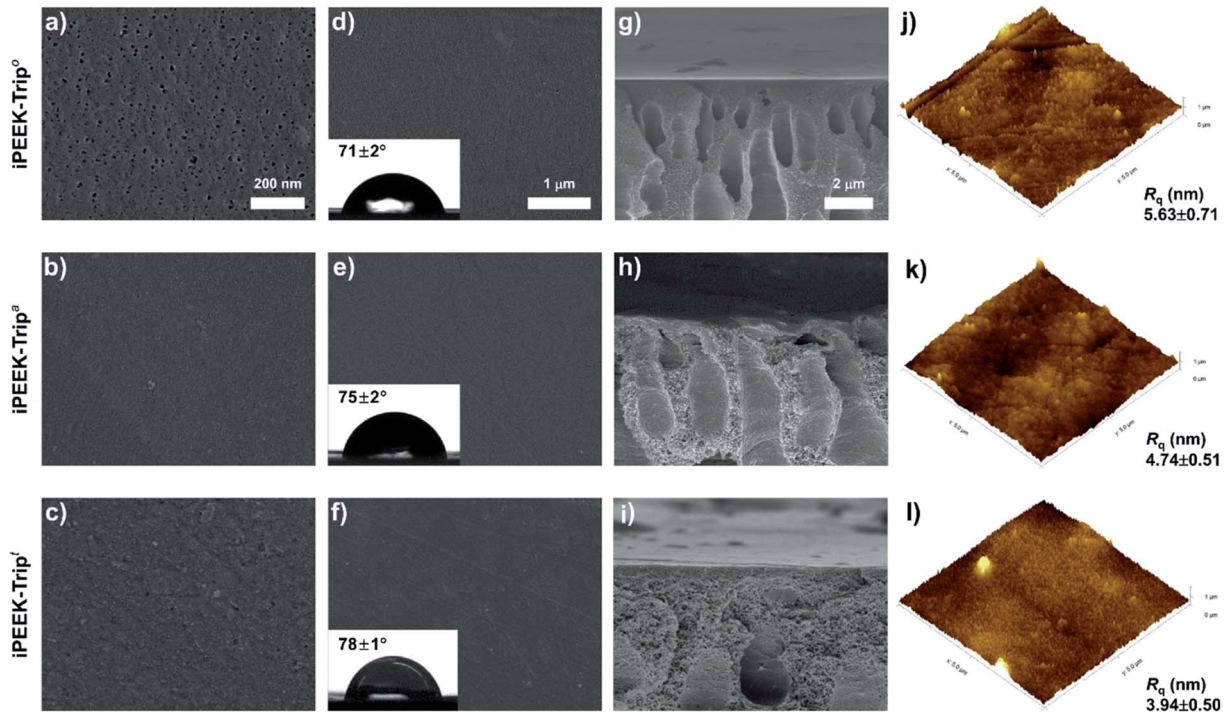

Fig. 3 Typical iPEEK membrane surface morphology at high (a–c) and low (d–f) magnifications, and cross-sectional images (g–i). The inset images are water contact angles (WCAs) of the membrane surface. Surface roughness shown by AFM images (j–l).

the highest reduced modulus of 1.1 GPa, followed by iPEEK-SBI^t with 0.89 GPa, and the lowest modulus was obtained for iPEEK-TB^t of 0.703 GPa. The hardness of all membranes lay between 0.005 GPa and 0.05 GPa. All membranes were sufficiently robust to be used for OSN at pressures up to 30 bar. The surface roughness of the membranes ranged between 4 and 9 nm (Table 2 and Fig. S25†).

The surface roughness decreased as the membranes became tighter within the same iPEEK series, and the water contact angle (WCA) increased simultaneously. Since the chemical structure of the polymer within a series was the same, the increase in WCA can be attributed to the decrease in the surface roughness.

Typical surface and cross-sectional morphologies of iPEEK membranes are shown in Fig. 3. The surface morphology revealed a uniform structure for all membranes. However, the cross-sectional images show that the finger-like macrovoid structures changed to sponge-like structures with an increase in the concentration of the dope solution (Fig. 3h–j). The viscous polymer dope solution delayed the formation of the asymmetric membrane during the phase inversion.[32] Therefore, the formation of the more dense surface morphology and sponge-like structures for iPEEK-Trip can be explained by the delayed demixing rate at high dope solution viscosity. The same trend and morphology changes were obtained for the two other polymers (iPEEK-SBI and iPEEK-TB), indicating the consistency of this process, as shown in Fig. S26–S28.†

Separation performance

The MWCO of the membranes was determined in acetonitrile at 30 bar (Fig. 4a, S29–S31†). The MWCO and the permeance decreased with increasing membrane tightness, *i.e.*, higher dope solution viscosity and concentration. In the case of iPEEK-SBI, the MWCO decreased from 770 to 450 g mol^{-1}. In contrast, the acetonitrile permeance decreased from 7.8 to 3.6 L m^{-2} h^{-1} bar^{-1} as a result of increasing the dope solution concentration from 27 wt% to 35 wt%, respectively. In general, the highest concentrations afforded the tightest membranes with MWCO values of 450, 480, and 528 g mol^{-1}, with corresponding permeance values of 3.6, 3.9, and 4.9 L m^{-2} h^{-1} bar^{-1} for iPEEK-SBI^t, iPEEK-TB^t, and iPEEK-Trip^t, respectively. In contrast, the lowest concentrations exhibited the most open membranes with MWCO values of 770, 845, and 820 g mol^{-1}, with corresponding permeance values of 7.8, 9.1, and 11.1 L m^{-2} h^{-1} bar^{-1} for iPEEK-SBI^o, iPEEK-TB^o, and iPEEK-Trip^o, respectively. The pore diameter distribution analysis revealed that the pore diameters were in the range of 0.84–0.90, 0.67–0.74, and 0.44–0.52 nm for the open, ajar, and tight membranes, respectively (Fig. 4b). The MWCO values showed good correlation with the pore size diameter, which was obtained from the pore flow model using the styrene rejection values.[33–35] The tightest membranes displayed lower MWCO and lower pore size diameters, and *vice versa* in the case of the more open membranes.

The tightness of the membranes was analyzed and expressed through their MWCO, permeance, and pore diameter, while the tightness of the new polymers was expressed by the FFV and BET surface area. A correlation between these parameters was

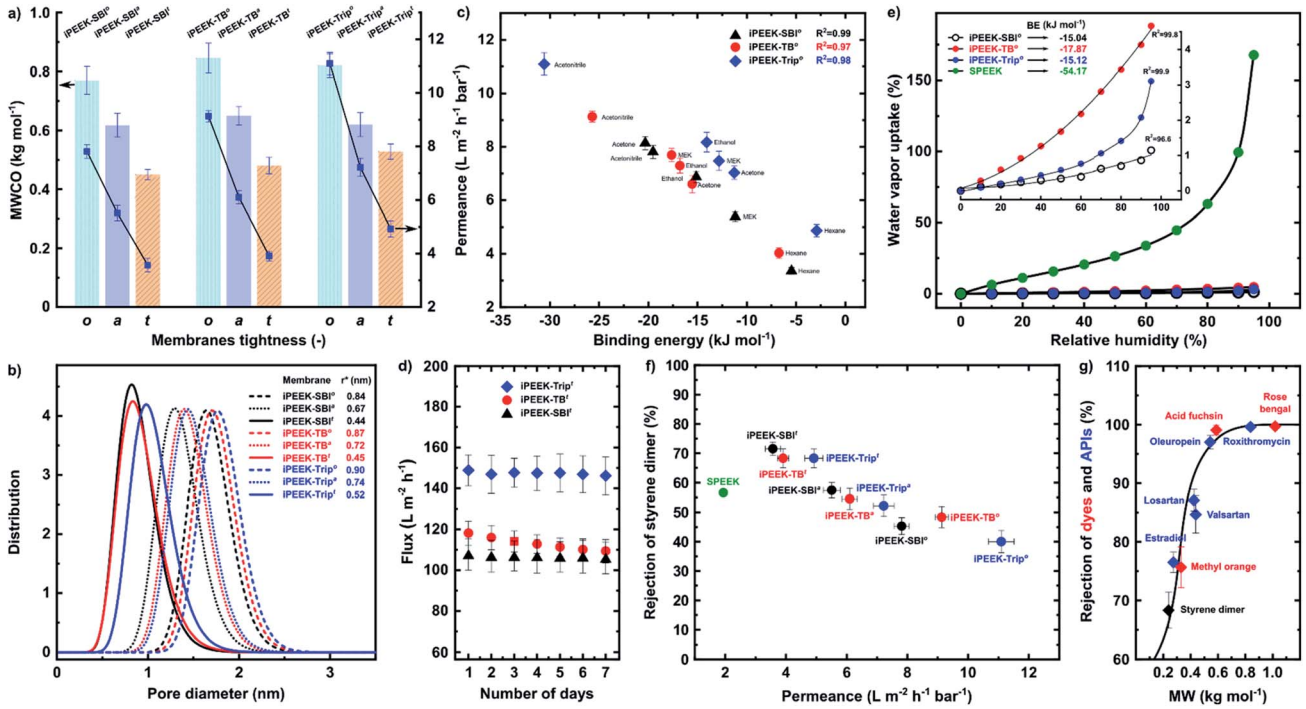

Fig. 4 (a) Molecular weight cutoff (MWCO) and permeance of the membranes. (b) Pore size distribution of the membranes. (c) Solvent permeances of the open membranes as a function of binding energies between the solvents and the polymers obtained from MD simulations. (d) Long-term stability during continuous operation of the tight membranes. Comparison of (e) the water vapor uptake as a function of relative humidity, (f) the nanofiltration performance for the novel iPEEKs and the previously reported SPEEK, and (g) rejection of some dyes and APIs on iPEEK-Trip^{t}. All nanofiltration experiments were carried out in acetonitrile at 30 bar using a cross-flow rig unless otherwise stated.

observed as the tightness of the membranes followed the tightness of the polymers; iPEEK-SBI, iPEEK-TB, and iPEEK-Trip polymers resulted in open, ajar, and tight membranes, respectively. Therefore, the MWCO, and subsequently the separation performance of the iPEEK membranes, can be fine-tuned either by adjusting the dope solution concentration or by incorporating different kinked structures.

Five solvents, with varying polarity, were used to further characterize the nanofiltration performance and stability of the membranes (Table S11†). The separation performance was directly related to the interactions between the solvents and the polymer matrix. These interactions were expressed through binding energies obtained from molecular dynamics simulations using Materials Studio (Fig. S32–S34, and Table S13†). The correlation between the solvent permeance and the binding energies is shown in Fig. 4c. As the absolute value of the binding energy between the solvents and the polymers increased, the solvent permeance increased. The non-polar hexane with the lowest absolute binding energy value displayed the lowest permeance of 3.4–4.9 L m^{-2} h^{-1} bar^{-1}. In contrast, the polar acetonitrile with the highest absolute binding energy value displayed the highest permeance up to 11.1 ± 0.4 L m^{-2} h^{-1} bar^{-1}. Consequently, in general, the higher the BE between the solvent and the polymer, the higher the permeance. As a function of BE, the swelling ratio of the membranes showed the same trend as the permeance; as the binding energy increased, the swelling ratio of the membranes increased linearly (Fig. S35–S39†). The solvent permeance was also plotted as a function of common solvent parameters, such as the Hansen Solubility Parameter (HSP) and the dielectric constant and density. However, no strong correlation was found (Fig. S48–S53†). Moreover, the membranes showed stable performance both at 10–30 bar (Fig. S40†) and over seven days of continuous cross-flow operation in acetonitrile under 30 bar (Fig. 4d).

Owing to the unavoidable presence of the –SO_3H moieties in the state-of-the-art SPEEK membrane obtained from commercial PEEK,[5] SPEEK displayed 33-fold (169%) higher water vapor uptake at 95% relative humidity with 3-fold higher binding energy than that of the iPEEKs (Fig. 4e). These results demonstrate that even a small percentage of undesired sulfonation from the solvent significantly changes the characteristics of the membrane. Among the new polymers, iPEEK-TB exhibited the highest water vapor sorption (4.6%) and binding energy (−17.9 kJ mol^{-1}) due to the presence of the tertiary amine group in the polymer matrix (Fig. S41 and Table S14†).[32] Fig. 4f shows the comparison of the performance of the iPEEK membranes with the reported SPEEK membrane.[5] The acetonitrile permeance of the iPEEK membranes was found to be 2–6 fold higher than that of the SPEEK. The iPEEK-SBI^{a} membrane exhibited the same rejection (57.4%) as SPEEK but the corresponding permeance was found to be 5.51 L m^{-2} h^{-1} bar^{-1}, which is 184% higher than that of SPEEK. Moreover, in comparison to SPEEK, both the rejection and the permeance for the iPEEK-SBI^{t} membrane increased by 26.4% and 84%, respectively.

In addition to the polystyrene rejections (Fig. S29–31†), three dyes and five active pharmaceutical ingredients (APIs) were also filtered using iPEEK-Trip^t in acetonitrile at 30 bar (Fig. 4g). The MWCO value was found to be approx. 420 g mol^{-1}, which is 20% lower than for the polystyrene markers (Fig. S31†). In general, these results indicate that polar solutes have higher rejection and the membranes are tighter.

Conclusions

In summary, three intrinsically porous poly(ether-ether-ketone) polymers (iPEEKs) were successfully designed, synthesized, and utilized for the fabrication of organic solvent nanofiltration (OSN) membranes. The polymers comprised triptycene, spirobisindane, and Tröger's base with contorted structures in their backbone. The obtained polymers successfully overcame the solution processability issues of commercial PEEK, displaying high thermal and chemical stability, and excellent mechanical flexibility. A notable boost in the fractional free volume and surface area was obtained. Fine-tuning of the iPEEK membrane separation performance was demonstrated, with molecular weight cutoff values in the range of 450–845 g mol^{-1}, by either varying the contorted structure or the dope solution concentration. Molecular dynamics simulations were successfully used to reveal the relationship between the polymer structures and the membrane performance. The long-term stability of the membranes was successfully demonstrated in five solvents at pressures up to 30 bar and up to seven days of continuous filtration. The presented work paves the way for molecular engineering of high-performance membranes.

Conflicts of interest

There are no conflicts to declare.

Acknowledgements

The research reported in this publication was supported by funding from King Abdullah University of Science and Technology (KAUST). The graphical abstract and Fig. 1 were created by Heno Hwang, scientific illustrator at KAUST. The postdoctoral fellowship from the Advanced Membranes and Porous Materials Center at KAUST is gratefully acknowledged (MAH, SHP, HV, and FHA).

Notes and references

1 G. Szekely, M. F. Jimenez-Solomon, P. Marchetti, J. F. Kim and A. G. Livingston, *Green Chem.*, 2014, **16**, 4440, DOI: 10.1039/C4GC00701H.
2 M.-L. Liu, J.-L. Guo, S. Japip, T.-Z. Jia, D.-D. Shao, S. Zhang, W.-J. Li, J. Wang, X.-L. Cao and S.-P. Sun, *J. Mater. Chem. A*, 2019, **7**, 3170, DOI: 10.1039/C8TA11372F.
3 K. Hendrix, G. Koeckelberghs and I. F. J. Vankelecom, *J. Membr. Sci.*, 2014, **452**, 241, DOI: 10.1016/j.memsci.2013.10.048.
4 J. da Silva Burgal, L. Peeva, P. Marchetti and A. Livingston, *J. Membr. Sci.*, 2015, **493**, 524, DOI: 10.1016/j.memsci.2015.07.012.
5 J. da Silva Burgal, L. Peeva, S. Kumbharkar and A. Livingston, *J. Membr. Sci.*, 2015, **479**, 105, DOI: 10.1016/j.memsci.2014.12.035.
6 J. da Silva Burgal, L. Peeva and A. Livingston, *Green Chem.*, 2016, **18**, 2374, DOI: 10.1039/C5GC02546J.
7 J. Silva Burgal, L. Peeva and A. Livingston, *J. Membr. Sci.*, 2017, **525**, 48, DOI: 10.1016/j.memsci.2016.10.015.
8 S. L. Aristizábal, S. Chisca, B. A. Pulido and S. P. Nunes, *Ind. Eng. Chem. Res.*, 2020, **59**, 5218, DOI: 10.1021/acs.iecr.9b04281.
9 A. Iulianelli and A. Basile, *Int. J. Hydrogen Energy*, 2012, **37**, 15241, DOI: 10.1016/j.ijhydene.2012.07.063.
10 L. C. H. Moh, J. B. Goods, Y. Kim and T. M. Swager, *J. Membr. Sci.*, 2018, **549**, 236, DOI: 10.1016/j.memsci.2017.11.041.
11 K. Hendrix, M. V. Eynde, G. Koeckelberghs and I. F. J. Vankelekom, *J. Membr. Sci.*, 2013, **447**, 212, DOI: 10.1016/j.memsci.2013.07.002.
12 N. B. McKeown and P. M. Budd, *Macromol*, 2010, **43**, 5163, DOI: 10.1021/ma1006396.
13 P. M. Budd, B. S. Ghanem, S. Makhseed, N. B. McKeown, K. J. Msayib and C. E. Tattershall, *Chem. Commun.*, 2004, **230**, DOI: 10.1039/B311764B.
14 P. M. Budd, in *Sustainable Nanoscale Engineering*, ed. G. Szekely and A. Livingston, Elsevier, 2020, p. 231. DOI: 10.1016/B978-0-12-814681-1.00009-6.
15 M. L. Jue, D.-Y. Koh, B. A. McCool and R. P. Lively, *Chem. Mater.*, 2017, **29**, 9863, DOI: 10.1021/acs.chemmater.7b03456.
16 Z.-X. Low, P. M. Budd, N. B. McKeown and D. A. Patterson, *Chem. Rev.*, 2018, **118**, 5871, DOI: 10.1021/acs.chemrev.7b00629.
17 N. B. McKeown, B. Ghanem, K. J. Msayib, P. M. Budd, C. E. Tattershall, K. Mahmood, S. Tan, D. Book, H. W. Langmi and A. Walton, *Angew. Chem., Int. Ed.*, 2006, **45**, 1804, DOI: 10.1002/anie.200504241.
18 Y. Wang, N. B. McKeown, K. J. Msayib, G. A. Turnbull and I. D. Samuel, *Sensors*, 2011, **11**, 2478, DOI: 10.3390/s110302478.
19 E. Madrid and N. B. McKeown, *Curr. Opin. Electrochem.*, 2018, **10**, 61, DOI: 10.1016/j.coelec.2018.04.008.
20 H. J. Mackintosh, P. M. Budd and N. McKeown, *J. Mater. Chem.*, 2008, **18**, 573, DOI: 10.1039/B715660J.
21 Z. Zhang, J. Zheng, K. Premasiri, M.-H. Kwok, Q. Li, R. Li, S. Zhang, M. H. Litt, X. P. A. Gao and L. Zhu, *Mater. Horiz.*, 2020, **7**, 592, DOI: 10.1039/C9MH01261C.
22 P. Gorgojo, S. Karan, H. C. Wong, M. F. Jimenez-Solomon, J. T. Cabral and A. G. Livingston, *Adv. Funct. Mater.*, 2014, **24**, 4729, DOI: 10.1002/adfm.201400400.
23 T. s. Anokhina, A. A. Yushkin, P. M. Budd and A. V. Volkov, *Sep. Purif. Technol.*, 2015, **156**, 683, DOI: 10.1016/j.seppur.2015.10.066.
24 S. Tsarkov, V. Khotimskiy, P. M. Budd, V. Volkov, J. Kukushkina and A. Volkov, *J. Membr. Sci.*, 2012, **423**, 65, DOI: 10.1016/j.memsci.2012.07.026.
25 D. Fritsch, P. Merten, K. Heinrich, M. Lazar and M. Priske, *J. Membr. Sci.*, 2012, **401**, 222, DOI: 10.1016/j.memsci.2012.02.008.
26 G. Ignacz, F. Fei and G. Szekely, *ACS Appl. Nano Mater.*, 2018, **1**, 6349, DOI: 10.1021/acsanm.8b01563.
27 M. Cook, P. R. j. Gaffney, L. G. Peeva and A. G. Livingston, *J. Membr. Sci.*, 2018, **558**, 52, DOI: 10.1016/j.memsci.2018.04.046.

28 J. Gao, S. Japip and T.-S. Chung, *Chem. Eng. J.*, 2018, **353**, 689, DOI: 10.1016/j.cej.2018.07.156.
29 D. Fritsch, P. Merten, K. Heinrich, M. Lazar and M. Priske, *J. Membr. Sci.*, 2012, **401**, 222, DOI: 10.1016/j.memsci.2012.02.008.
30 S. Zhou, Y. Zhao, J. Zheng and S. Zhang, *J. Membr. Sci.*, 2019, **591**, 117347, DOI: 10.1016/j.memsci.2019.117347.
31 M. A. Abdulhamid, X. Ma, X. Miao and I. Pinnau, *Polym.*, 2017, **130**, 182, DOI: 10.1016/j.polymer.2017.10.017.
32 A. K. Hołda and I. F. J. Vankelecom, *J. Appl. Polym. Sci.*, 2015, **132**, 42130, DOI: 10.1002/app.42130.
33 J. Stawikowska, J. F. Kim and A. G. Livingston, *Chem. Eng. Sci.*, 2013, **97**, 81, DOI: 10.1016/j.ces.2013.03.054.
34 W. R. Bowen and J. S. Welfoot, *Chem. Eng. Sci.*, 2002, **57**, 1393, DOI: 10.1016/S0009-2509(01)00412-2.
35 F. Fei, H. A. L. Phuong, C. F. Blanford and G. Szekely, *ACS Appl. Polym. Mater.*, 2019, **1**, 452, DOI: 10.1021/acsapm.8b00161.